

Neutron macromolecular crystallography with
LADI-III

Matthew P. Blakeley,^{a*}
Susana C. M. Teixeira,^{b,c} Isabelle
Petit-Haertlein,^{a,b} Isabelle
Hazemann,^d Andre Mitschler,^d
Michael Haertlein,^{a,b} Eduardo
Howard^e and Alberto D.
Podjarny^{d*}

^aInstitut Laue–Langevin, 6 Rue Jules Horowitz,
38042 Grenoble, France, ^bILL–EMBL
Deuteration Laboratory, Partnership for
Structural Biology, 6 Rue Jules Horowitz,
38042 Grenoble, France, ^cEPSAM, Keele
University, Staffordshire ST5 5BG, England,
^dIGBMC, CNRS, INSERM, Université de
Strasbourg, 1 Rue Laurent Fries, Illkirch, France,
and ^eIFLYSIB, CONICET, Calle 59, 789 La Plata,
Argentina

Correspondence e-mail: blakeleym@ill.fr,
podjarny@igbmc.fr

At the Institut Laue–Langevin, a new neutron Laue diffractometer LADI-III has been fully operational since March 2007. LADI-III is dedicated to neutron macromolecular crystallography at medium to high resolution (2.5–1.5 Å) and is used to study key H atoms and water structure in macromolecular structures. An improved detector design and readout system has been incorporated so that a miniaturized reading head located inside the drum scans the image plate. From comparisons of neutron detection efficiency (DQE) with the original LADI-I instrument, the internal transfer of the image plates and readout system provides an approximately threefold gain in neutron detection. The improved performance of LADI-III, coupled with the use of perdeuterated biological samples, now allows the study of biological systems with crystal volumes of 0.1–0.2 mm³, as illustrated here by the recent studies of type III antifreeze protein (AFP; 7 kDa). As the major bottleneck for neutron macromolecular studies has been the large crystal volumes required, these recent developments have led to an expansion of the field, extending the size and the complexity of the systems that can be studied and reducing the data-collection times required.

Received 15 April 2010

Accepted 26 May 2010

1. Introduction

The importance of X-ray diffraction techniques for the determination of macromolecular structures cannot be over-emphasized. Currently, around 59 000 X-ray structures have been deposited in the Protein Data Bank (<http://www.rcsb.org/pdb>) and these have contributed significantly to our understanding of a vast array of biological processes and systems. However, the great majority of these X-ray macromolecular structures provide us with no, or very little, information relating to the positions of the H atoms owing to the fact that H atoms, with only one electron, scatter X-rays very weakly. The difficulty in identifying H atoms within electron-density maps is further exacerbated by their degree of thermal motion, such that labile H atoms (B factors $> 10 \text{ \AA}^2$) are extremely difficult to visualize even when ultrahigh-resolution data are available ($< 1.2 \text{ \AA}$; Howard *et al.*, 2004). In contrast, in neutron crystallography the scattering centres are the atomic nuclei and as such the neutron scattering lengths show no correlation to the number of electrons but rather depend on the nuclear forces, which can vary even between different isotopes of the same element. H and/or D atoms can be more readily located using neutron diffraction techniques because the scattering lengths of hydrogen ($-0.374 \times 10^{-12} \text{ cm}$) and deuterium ($+0.667 \times 10^{-12} \text{ cm}$) are comparable to those of the other atoms of a macromolecule, *i.e.* C ($+0.665 \times 10^{-12} \text{ cm}$), N ($+0.937 \times 10^{-12} \text{ cm}$), O ($+0.580 \times 10^{-12} \text{ cm}$) and S ($+0.280 \times$

10^{-12} cm). This 'high visibility' of H and D atoms in neutron crystallography allows their positions to be determined at resolutions of ~ 1.5 and 2.5 Å, respectively (Blakeley, 2009). Neutron crystallography can therefore complement X-ray structure determination by providing a more complete description of the structure. This has been exploited in studies of enzyme mechanism, in which the location of H atoms in the active site and knowledge of the protonation states of amino-acid residues can help to decipher the mechanisms involved (Blakeley *et al.*, 2008; Coates *et al.*, 2008; Adachi *et al.*, 2009; Kovalevsky *et al.*, 2010; Tomanicek *et al.*, 2010), in ligand/inhibitor-binding studies in order to identify the hydrogen-bonding interactions which occur (Wlodawer *et al.*, 1983; Coates *et al.*, 2001; Kovalevsky *et al.*, 2008) and in studies of bound solvent structure (Bon *et al.*, 1999; Habash *et al.*, 2000; Blakeley *et al.*, 2004; Chatake *et al.*, 2005; Arai *et al.*, 2005), in which the positions and orientations of water molecules (as D_2O) can be determined, providing detailed distance and angle information relating to hydrogen bonding and allowing us to visualize the networks that are formed (Bouquiere *et al.*, 1993; Blakeley *et al.*, 2004). Furthermore, the difference in magnitude and phase between hydrogen and deuterium means that neutron diffraction can determine the pattern and extent of H/D-isotope substitution in macromolecules, providing information on the solvent accessibility of individual amino acids, on the mobility and flexibility of interesting domains and on the H/D-exchange dynamics themselves (Wlodawer & Sjolín, 1982; Mason *et al.*, 1984; Kossiakoff *et al.*, 1991; Bennett *et al.*, 2008).

Despite the wealth of information that can be derived from neutron crystallography, there are currently only 41 deposited macromolecular neutron structures in the Protein Data Bank (<http://www.rcsb.org/pdb>). This is a consequence of difficulties associated with neutron macromolecular crystallography that make a successful experiment a lot more demanding than its X-ray counterpart. The principal problem is that even the most intense neutron sources have fluxes which are many orders of magnitude lower than the corresponding fluxes of X-ray beams. Historically, therefore, it has been a necessity to have an extremely large crystal (~ 10 mm³) and to count for long times (months) in order to gain sufficiently high reflection intensities (Wlodawer, 1980). These long data-collection times were also a consequence of a lack of optimized instrumentation for neutron macromolecular crystallography, with data being collected using monochromatic thermal neutron beams on four-circle or flat-cone diffractometers fitted with small linear or area ³He position-sensitive detectors. This restricted neutron studies to just a few macromolecules for which extremely large crystal volumes could be grown and which possess relatively small unit-cell volumes.

2. Neutron image plates and quasi-Laue methods with cold neutrons

In the early 1990s, important advances were made in neutron macromolecular crystallography which extended the field towards larger systems while using smaller crystals and shorter

data-collection times. The development of neutron-sensitive image plates (NIPs) for use as a cylindrical detector (Rausch *et al.*, 1992; Wilkinson *et al.*, 1992; Cipriani *et al.*, 1994) provided a much larger coverage of reciprocal space than had previously been possible. This allowed many more reflections to be measured at once and thus helped to reduce the data-collection times necessary. An NIP is very similar to an X-ray image plate in that it consists of photo-stimulable luminescent materials and is sensitive to X-rays and γ -rays. However, in order to make the image plate sensitive to neutrons, a neutron scintillator such as gadolinium (Gd) must be added. NIPs can be produced by mixing the neutron converter Gd_2O_3 with a photo-stimulable luminescent material (BaFBr doped with Eu^{2+} ions) on a plastic support (Niimura *et al.*, 1994) and are comparatively cheap and capable of high spatial resolution (~ 0.1 – 0.2 mm); they have good homogeneity, a large dynamical range ($1:10^5$), extended linearity and possess no dead-time or electronic noise build-up with time.

Another important development was the introduction of quasi-Laue methods for neutron data collection (Wilkinson & Lehmann, 1991). By using Ni/Ti multilayer band-pass filters of high reflectivity (Schoenborn, 1992; Høghøj *et al.*, 1996), a restricted wavelength band is extracted from the white beam such that the flux is increased relative to monochromatic data-collection methods, while at the same time reducing background scattering and reflection overlap compared with use of the full white beam. The sample is then exposed to all available neutrons within the selected band pass, producing a much larger number of reflections than with a monochromatic neutron beam. Moreover, by having various Ni/Ti multilayer filters with different wavelength ranges ($\delta\lambda/\lambda$) and centred at different wavelengths (λ) one can optimize data collection by selecting the wavelength range ($\delta\lambda/\lambda$) and wavelength (λ) that are best suited to the sample (in terms of the unit-cell volume, crystal volume *etc.*). With the development of cold sources at neutron reactors and the larger coverage of reciprocal space offered by the use of cylindrical image-plate detectors, *i.e.* full back-scattering possibilities, longer wavelength cold neutrons can now be used for neutron macromolecular data collection. The main advantage of using longer wavelength neutrons is that the intensity of a reflection is proportional to the square of the incident neutron wavelength, so that for weakly scattering samples such as macromolecular crystals the reflection intensities can be increased, aiding the resolution limit of the data.

3. perdeuteration

An important factor that must be considered when studying biological macromolecules with neutrons is the very large incoherent scattering cross-section of hydrogen (80.27 barns; 1 barn = 10^{-24} cm⁻²). As H atoms account for around half of the atoms in a macromolecule, an extremely large incoherent signal is observed which severely limits the signal-to-noise ratio of the data and hence the resolution limit. Deuterium, on the other hand, has a much lower incoherent scattering cross-section (2.05 barns) and so it is advantageous to exchange the

H atoms in the crystal for D atoms. Traditionally, this has been achieved by growing crystals from or soaking the crystals in D₂O solutions, exchanging solvent-accessible groups (*e.g.* amino and hydroxyl groups), which typically amount to 15–20% of the solvent-accessible hydrogen content of the macromolecule (Myles, 2006). The only method of replacing all of the H atoms is to produce a completely perdeuterated macromolecule *in vivo* (Berns, 1963; Gamble *et al.*, 1994; Shu *et al.*, 2000; Hazemann *et al.*, 2005). To achieve this, the macromolecule must be expressed from bacteria grown on deuterated media so that perdeuterated macromolecules can be synthesized. For the growth of well ordered perdeuterated crystals, it is important to note that it may be necessary to re-optimize the crystallization conditions used for protiated crystals owing to differences in the physico-chemical properties of D₂O and H₂O, which affect protein–solvent and protein–protein interactions and hence the protein solubility (Budayova-Spano *et al.*, 2007). Moreover, it is also important to verify that the exchange of H for D does not affect the macromolecular structure (Fisher & Helliwell, 2008). Several X-ray studies have compared the crystal structures derived from protiated and perdeuterated crystals, with no significant differences being observed (Cooper *et al.*, 1998; Tuominen *et al.*, 2004; Artero *et al.*, 2005; Meilleur *et al.*, 2005; Budayova-Spano *et al.*, 2006; Di Costanzo *et al.*, 2007). Nevertheless, a comparison of the structures should be performed for each study, as it is possible that the differing crystallization conditions may affect the overall structures, as was the case for protiated and perdeuterated haloalkane dehalogenase (Liu *et al.*, 2007).

The use of perdeuterated crystals in recent years has been one of the major developments in neutron macromolecular crystallography. The main advantage of perdeuteration is that it permits the use of much smaller crystal volumes: at least an order of magnitude smaller (Hazemann *et al.*, 2005) relative to D₂O-soaked (or D₂O-grown) protiated crystals. Since the growth of very large single crystals is the major bottleneck in neutron macromolecular crystallography, this reduction in crystal volume requirements is of critical importance.

At the resolutions currently attainable for neutron macromolecular studies ($\sim 1.5\text{--}2.5$ Å), when using protiated crystals (grown or soaked in D₂O) the possibility always exists of the cancellation of nuclear density between an H atom and the positively scattering atom to which it is bound, *e.g.* C–H or O–H, which can lead to difficulties in interpretation of the neutron data. In contrast, as deuterium has a positive coherent scattering length, with perdeuterated crystals this cancellation of nuclear density does not arise and hence the quality of the nuclear scattering density maps is improved. Moreover, for protiated crystals (grown or soaked in D₂O) the possibility of partial occupancy of H and D atoms always exists; with perdeuterated crystals this ambiguity is removed.

Despite the many advantages perdeuteration offers, until relatively recently it has been exploited rather less than might have been expected. In 2003, the ILL, in collaboration with the EMBL Grenoble Outstation, were the first to create a ‘Deuteration Laboratory’ (Forsyth *et al.*, 2001) aimed at

maximizing the effectiveness of biological neutron scattering work. Since then, other neutron facilities throughout the world have developed specific laboratories for the deuteration of macromolecules, such as the Bio-Deuteration Laboratory at Oak Ridge National Laboratory (ORNL), the Biological Deuteration Laboratory at LANSCE and the Biodeuteration Facility at the Australian Nuclear Science and Technology Organization (ANSTO).

4. The Laue diffractometers: LADI-I and VIVALDI

The potential gains for neutron macromolecular crystallography in harnessing the use of quasi-Laue methods with cold neutrons and a large cylindrical NIP detector led to the construction of the first neutron Laue diffractometer ‘LADI-I’ at the Institut Laue–Langevin in collaboration with the European Molecular Biology Laboratory (EMBL) Grenoble Outstation (Cipriani *et al.*, 1996; Myles *et al.*, 1998). The LADI-I instrument was used to collect data from several macromolecules, including xylose isomerase (Meilleur *et al.*, 2006), endothiasepsin (Coates *et al.*, 2001), lysozyme (Niimura *et al.*, 1997; Bon *et al.*, 1999), concanavalin A (Habash *et al.*, 2000; Blakeley *et al.*, 2004) and aldose reductase (Blakeley *et al.*, 2006, 2008). The impact of perdeuteration on neutron macromolecular crystallography, in terms of the smaller crystal volume requirements, was demonstrated by studies on aldose reductase (Hazemann *et al.*, 2005), for which neutron data to 2.2 Å resolution were collected on LADI-I from a perdeuterated crystal with a volume of only 0.15 mm³, which was radically smaller than any crystal previously used for neutron macromolecular crystallography. Moreover, using protocols developed for the successful cryocooling of large macromolecular crystals, neutron diffraction data could be collected at cryotemperatures using LADI-I (Blakeley *et al.*, 2004), opening up the way for studies of freeze-trapped intermediates.

Owing to the success of the LADI-I instrument, the possibility of using quasi-Laue methods with thermal rather than cold neutrons for fast data collection from much smaller unit-cell systems was investigated. These trials were shown to be a success and led to the construction and subsequent installation in 2001 of a second Laue diffractometer, originally called ‘LADI-II’ but later renamed ‘VIVALDI’ (Very Intense Vertical Axis Laue Diffractometer; Wilkinson *et al.*, 2002). Unlike LADI-I, which uses a horizontal cylindrical drum detector with externally bonded image plates and readout, VIVALDI uses a cylindrical drum detector in a vertical configuration and has neutron image plates that are mounted and read internally, so that the side of the image plate that receives diffracted neutrons is the same as that from which the photo-stimulated luminescence is read. This was shown to improve the neutron detection efficiency of VIVALDI by a factor of ~ 3 in comparison to LADI-I. Thus, in 2003, as part of the ILL Millennium Programme, a project was initiated to build an upgraded Laue diffractometer ‘LADI-III’ based on the design of VIVALDI and as a replacement for the LADI-I instrument.

5. The Laue diffractometer LADI-III

Similar to VIVALDI, the LADI-III instrument (Fig. 1) has a vertical configuration and the image plates and read/erase system are located internally. In addition, further important modifications to the design have been incorporated, such as an increase in the size of the cylindrical drum detector (to 400 mm in diameter with a height of 450 mm) and a reduction in the size of the internal read/erase system. The drum diameter was increased so as to reduce the number of spatially overlapped reflections and to decrease the background scatter per pixel, while the miniaturized design of the read/erase system allows increased coverage of reciprocal space by minimizing the image-plate dead zone. Moreover, the design allows the instrument to be installed on any inclined beam of up to 2° and on any beam height from 630 to 1400 mm, such that relocation to a higher flux beam position is possible, with this being scheduled to happen in 2011. Commissioning of the LADI-III instrument was completed in early 2007 and since

March 2007 it has been fully operational and open to scientists. The crystal (in a quartz capillary) is mounted on a goniometer and placed inside the cylindrical drum, where it can be rotated around the cylinder axis. Data are collected by resetting the crystal sample by $\sim 5^\circ$ between each successive exposure. Interaction of the neutron beam with the sample produces Bragg reflections, which are recorded on neutron image plates bonded to the inner surface of the vertical cylindrical drum. The internal reading system scans the drum in phonographic mode. For the majority of systems studied, a multilayer band-pass filter of $\delta\lambda/\lambda = 25\%$ centred at $\lambda = 3.5 \text{ \AA}$ is used for data collection. The resolution at the edge of the detector is then $\sim 1.5 \text{ \AA}$, which is sufficient to localize protons and deuterons. However, for a large unit-cell system ($a > 110 \text{ \AA}$), where a large number of reflections are simultaneously produced, use of a narrower band-pass multilayer filter (e.g. $\delta\lambda/\lambda$ of 5–10%) helps to reduce the problem of spatial overlap. For smaller unit-cell systems ($a < 50 \text{ \AA}$) much wider band-pass multilayer filters can be used (e.g. $\delta\lambda/\lambda = 35\%$) in order to improve data-

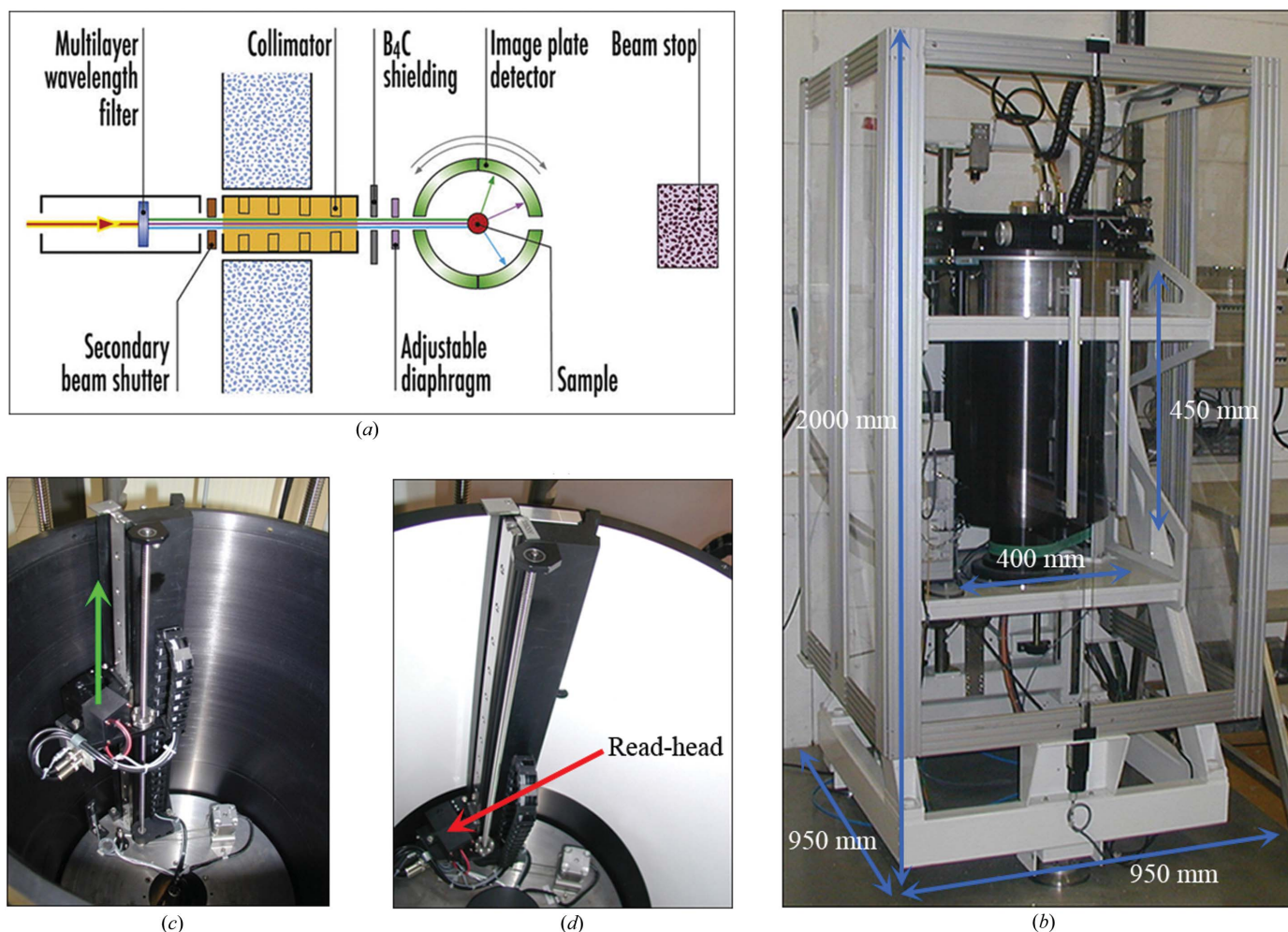


Figure 1

The LADI-III Laue diffractometer at the Institut Laue–Langevin. (a) Schematic of the instrument layout. (b) The LADI-III instrument installed on cold guide H142 with the overall dimensions of the instrument shown. (c) The inside of the drum with the reading head shown tracking-up while the drum itself rotates. The green arrow indicates the direction of the reading head. (d) The inside of the detector, with the bonded neutron image plates and the reading system in the position during exposure (shown by the red arrow).

Table 1

Neutron quasi-Laue data-collection statistics for hen egg-white lysozyme using the neutron diffractometers LADI-I and LADI-III.

Values in parentheses are for the highest resolution shell.

Neutron source	Institut Laue–Langevin	Institut Laue–Langevin
Guide	Cold neutron guide H142	Cold neutron guide H142
Instrument	LADI-I	LADI-III
Wavelength (Å)	2.9–4.3	2.9–4.3
No. of images	9	9
Image width	Stationary	Stationary
Setting spacing (°)	4	4
Exposure time (h)	4	4
Space group	$P4_32_12$	$P4_32_12$
Unit-cell parameters (Å, °)	$a = 79.1, b = 79.1, c = 38.1, \alpha = 90, \beta = 90, \gamma = 90$	$a = 79.1, b = 79.1, c = 38.1, \alpha = 90, \beta = 90, \gamma = 90$
Resolution range (Å)	22.55–2.00 (2.11–2.00)	22.55–2.00 (2.11–2.00)
No. of observations	8398 (622)	29337 (2374)
No. of unique reflections	4626 (381)	5978 (668)
Completeness (%)	55.9 (31.9)	71.8 (56.1)
R_{merge}^\dagger	0.150 (0.186)	0.177 (0.198)
$R_{\text{p.i.m.}}^\ddagger$ (all I^+ and I^-) \ddagger	0.106 (0.144)	0.068 (0.092)
Mean $I/\sigma(I)$	5.1 (4.4)	7.8 (5.6)
Multiplicity	1.8 (1.6)	4.9 (3.6)

$^\dagger R_{\text{merge}} = \sum_{hkl} \sum_i |I_i(hkl) - \langle I(hkl) \rangle| / \sum_{hkl} \sum_i I_i(hkl)$, where $I(hkl)$ is the intensity of reflection hkl , \sum_{hkl} is the sum over all reflections and \sum_i is the sum over i measurements of reflection hkl . $^\ddagger R_{\text{p.i.m.}} = \sum_{hkl} [1/(N-1)]^{1/2} \sum_i |I_i(hkl) - \langle I(hkl) \rangle| / \sum_{hkl} \sum_i I_i(hkl)$ (Weiss, 2001), where $I(hkl)$ is the intensity of reflection hkl , \sum_{hkl} is the sum over all reflections and \sum_i is the sum over i measurements of reflection hkl .

collection efficiency. Furthermore, the band-pass filters can be ‘tuned’ so that they can be centred at shorter wavelengths, offering the possibility of collecting higher resolution data.

In order to compare the quality of the data collected using LADI-I and LADI-III, diffraction experiments were performed on both diffractometers using the same tetragonal hen egg-white lysozyme crystal and data-collection parameters, *i.e.* neutron flux, aperture size, wavelength range, exposure time and angular setting spacing between successive images. The results indicate, as expected, that the data collected from LADI-III are of higher accuracy (lower $R_{\text{p.i.m.}}$ values), have improved signal-to-noise ratios [mean $I/\sigma(I)$], have a lower degree of spatial overlap and are more complete (Table 1). Furthermore, data can be collected in faster times, from smaller crystal volumes and to higher resolution. The detective quantum efficiencies (DQEs) for both LADI-I and LADI-III have been calculated by analysing the background regions of diffraction patterns collected from a DNA crystal. The DQEs for LADI-I and LADI-III were found to be 16 and 46%, respectively (Wilkinson *et al.*, 2009), corroborating the results from the comparative tests with the lysozyme crystal.

The neutron quasi-Laue diffraction data are processed using software from Daresbury Laboratory (Warrington, England; Helliwell *et al.*, 1989; Campbell, 1995) modified for the cylindrical detector geometry and with the polarization correction removed (Campbell *et al.*, 1998). The initial stages of processing quasi-Laue data, such as indexing, orientation matrix and spot parameter refinement and reflection integration, are performed using the *LAUEGEN* program (Campbell *et al.*, 1998), while *LSCALE* (Arzt *et al.*, 1999) is used to derive

Table 2

Neutron quasi-Laue data-collection statistics for the perdeuterated AFP crystal with volume 0.13 mm³.

Values in parentheses are for the highest resolution shell.

Neutron source	Institut Laue–Langevin
Guide	Cold neutron guide H142
Instrument	LADI-III
Wavelength (Å)	3.18–4.22
No. of images	82
Image width	Stationary
Setting spacing (°)	7
Average exposure time (h)	6.15
Space group	$P2_12_12_1$
Unit-cell parameters (Å, °)	$a = 32.7, b = 39.1, c = 46.5, \alpha = 90, \beta = 90, \gamma = 90$
Resolution range (Å)	32.74–1.85 (1.95–1.85)
No. of observations	71182 (3133)
No. of unique reflections	4803 (544)
Completeness (%)	89.3 (71.4)
R_{merge}^\dagger	0.140 (0.195)
$R_{\text{p.i.m.}}^\ddagger$ (all I^+ and I^-) \ddagger	0.031 (0.069)
Mean $I/\sigma(I)$	17.5 (5.5)
Multiplicity	14.8 (5.8)

$^\dagger R_{\text{merge}} = \sum_{hkl} \sum_i |I_i(hkl) - \langle I(hkl) \rangle| / \sum_{hkl} \sum_i I_i(hkl)$, where $I(hkl)$ is the intensity of reflection hkl , \sum_{hkl} is the sum over all reflections and \sum_i is the sum over i measurements of reflection hkl . $^\ddagger R_{\text{p.i.m.}} = \sum_{hkl} [1/(N-1)]^{1/2} \sum_i |I_i(hkl) - \langle I(hkl) \rangle| / \sum_{hkl} \sum_i I_i(hkl)$ (Weiss, 2001), where $I(hkl)$ is the intensity of reflection hkl , \sum_{hkl} is the sum over all reflections and \sum_i is the sum over i measurements of reflection hkl .

the wavelength-normalization curve by using the intensities of symmetry-equivalent reflections measured at different wavelengths.

The Institut Laue–Langevin is located on the same site as both the EMBL Grenoble Outstation and the European Synchrotron Radiation Facility (ESRF). Owing to the lack of radiation damage, crystals used for neutron data collection on LADI-III can be used immediately afterwards for data collection using X-rays. These data can then be combined for use in a joint X-ray and neutron refinement strategy (Adams *et al.*, 2009; Afonine *et al.*, 2010) using either *phenix.refine* from the *PHENIX* software package (available from <http://www.phenix-online.org>) or the *nCNS* software available from <http://mnc.lanl.gov>.

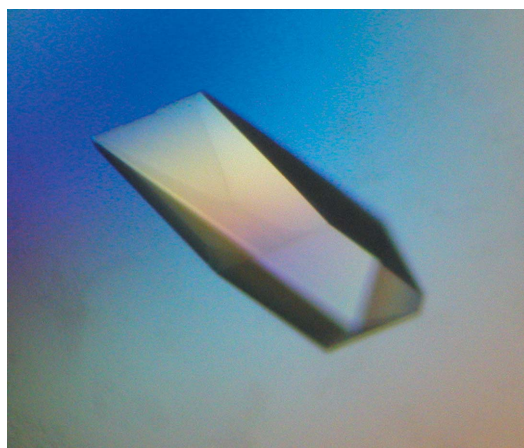


Figure 2

The perdeuterated crystal of AFP with dimensions 0.35 × 0.55 × 0.7 mm corresponding to a volume of 0.13 mm³ (Petit-Haertlein *et al.*, 2009).

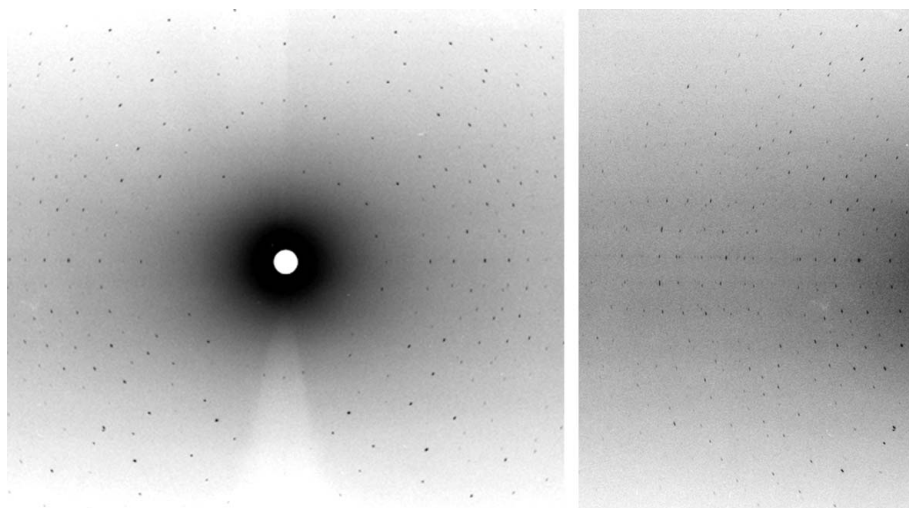


Figure 3 Left, centre section of a neutron quasi-Laue diffraction pattern from the 0.13 mm^3 perdeuterated AFP crystal obtained using LADI-III and a 24 h exposure time. Right, close-up of a high-resolution region.

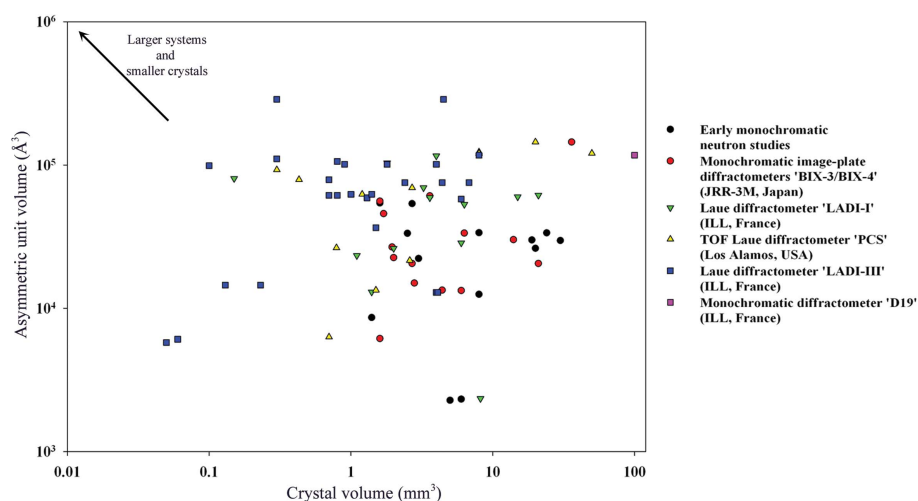


Figure 4 Plot of the asymmetric unit-cell volume (\AA^3) versus the crystal volume (mm^3) for the neutron structures solved to date on the various diffractometers available both past and present. The newer instruments such as the Protein Crystallography Station (PCS) and LADI-III are able to collect data from larger asymmetric unit cells and using smaller crystal volumes. The original necessity of having a crystal volume of several cubic millimetres is no longer the case, with data now being collected from perdeuterated protein crystals with volumes of $\sim 0.1 \text{ mm}^3$ and from D_2O -soaked protiated crystals with volumes much less than 1 mm^3 .

Several neutron data sets have now been collected on LADI-III with joint X-ray and neutron structural refinements under way or completed (Weiss *et al.*, 2008; Teixeira *et al.*, 2008; Gardberg *et al.*, 2009, 2010; Oksanen *et al.*, 2009; Leal *et al.*, 2009; Tomanicek *et al.*, 2010; Novak *et al.*, 2009; Petit-Haertlein *et al.*, 2009, 2010). Demand for the instrument is high (it is oversubscribed by a factor of three), with more than half of the users producing perdeuterated samples by taking advantage of the Deuteration Laboratory facility (Forsyth *et al.*, 2001).

Several data sets have been collected at LADI-III using D_2O -soaked protiated crystals with volumes of much less than 1 mm^3 and from perdeuterated crystals with volumes of $\sim 0.1\text{--}0.2 \text{ mm}^3$. This is a major step in overcoming

6. Neutron diffraction studies of type III antifreeze protein

An example of a recent neutron study performed using LADI-III which illustrates the improved capabilities of the new instrument combined with the use of perdeuterated biological samples is that of type III antifreeze protein. The members of the homologous type III antifreeze protein (AFP) subfamily share the capability to inhibit ice growth that would otherwise be fatal to organisms that live in subzero environments. AFPs work by binding to ice-crystal nuclei and although interactions between a defined flat ice-binding surface and a particular lattice plane of an ice crystal have been identified, the fine structural features that underlie the antifreeze mechanism still remain unclear. Despite the many extensive X-ray structural studies that have been carried out to date, additional work is required both at the residue-protonation and hydration levels in order to completely elucidate the antifreeze mechanism. Neutron diffraction data have been collected using LADI-III at 293 K from a crystal of perdeuterated antifreeze protein with dimensions of $0.35 \times 0.55 \times 0.7 \text{ mm}$ (Fig. 2), corresponding to a volume of 0.13 mm^3 (Petit-Haertlein *et al.*, 2009). Using exposure times ranging from 2 to 24 h, neutron diffraction data were collected to 1.85 \AA resolution (Fig. 3), with the complete data set being collected in three weeks. Data-reduction statistics are summarized in Table 2.

7. Conclusions

The impact of neutron macromolecular crystallography has recently increased, as it has provided information about key biological processes such as enzymatic mechanisms. Two main factors have contributed to this increase: the improvement in data-collection facilities and the use of perdeuterated samples, which improve the signal strength and reduce data-collection times. LADI-III is a clear example of the improvement in data-collection facilities. The difference from LADI-I is clearly seen in Table 1 and Fig. 4.

the important bottleneck of increasing the crystal volume in order to measure neutron diffraction data. Fig. 4 also shows a comparison with other existing data-collection facilities such as the 'biological crystal diffractometers' BIX-3 and BIX-4 at Tokai, Japan and the Protein Crystallography Station (PCS) at Los Alamos, USA. There is a clear trend towards larger systems and smaller crystals. This trend should continue with the new instrumentation for neutron macromolecular crystallography at the Spallation Neutron Source (SNS) at Oak Ridge National Laboratory and the Japan Proton Accelerator Research Complex (J-PARC).

The case of perdeuterated AFP shows the impact of both perdeuteration and the use of the LADI-III instrument on the quality of the data. High-resolution data (1.85 Å) have been collected from a very small crystal (0.13 mm³) in three weeks with high completeness, good agreement factors, high multiplicity and high signal-to-noise ratios. This opens the way to a more extended use of neutron macromolecular crystallography by the structural biology community.

This work was supported by the Human Frontiers Science Program grant RGP0021/2006-C and benefited from the activities of the DLAB consortium funded by the European Union under contract HPRI-2001-50065 and from United Kingdom Engineering and Physical Sciences Research Council (EPSRC)-funded activity within the ILL-EMBL Deuteration Laboratory under grant GR/R99393/01. EIH is member of the 'Carrera del Investigador' Conicet-Argentina. This work was supported by the Centre National de la Recherche Scientifique (CNRS), the Institut National de la Santé et de la Recherche Médicale and the Hôpital Universitaire de Strasbourg (HUS). The construction of the LADI-III diffractometer was financed by a grant from the European Commission [Grant No. 011995 CISB (RICN)].

References

- Adachi, M. *et al.* (2009). *Proc. Natl Acad. Sci. USA*, **106**, 4641–4646.
- Adams, P. D., Mustyakimov, M., Afonine, P. V. & Langan, P. (2009). *Acta Cryst.* **D65**, 567–573.
- Afonine, P. V., Mustyakimov, M., Grosse-Kunstleve, R. W., Moriarty, N. W., Langan, P. & Adams, P. D. (2010). *Acta Cryst.* **D66**, 1153–1163.
- Arai, S., Chatake, T., Ohhara, T., Kurihara, K., Tanaka, I., Suzuki, N., Fujimoto, Z., Mizuno, H. & Niimura, N. (2005). *Nucleic Acids Res.* **33**, 3017–3024.
- Artero, J.-B., Härtlein, M., McSweeney, S. & Timmins, P. (2005). *Acta Cryst.* **D61**, 1541–1549.
- Arzt, S., Campbell, J. W., Harding, M. M., Hao, Q. & Helliwell, J. R. (1999). *J. Appl. Cryst.* **32**, 554–562.
- Bennett, B. C., Gardberg, A. S., Blair, M. D. & Dealwis, C. G. (2008). *Acta Cryst.* **D64**, 764–783.
- Berns, D. S. (1963). *Biochemistry*, **6**, 1377–1380.
- Blakeley, M. P. (2009). *Crystallogr. Rev.* **15**, 157–218.
- Blakeley, M. P., Kalb, A. J., Helliwell, J. R. & Myles, D. A. A. (2004). *Proc. Natl Acad. Sci. USA*, **101**, 16405–16410.
- Blakeley, M. P., Mitschler, A., Hazemann, I., Meilleur, F., Myles, D. A. A. & Podjarny, A. D. (2006). *Eur. Biophys. J.* **35**, 577–583.
- Blakeley, M. P., Ruiz, F., Cachau, R., Hazemann, I., Meilleur, F., Mitschler, A., Ginell, S., Afonine, P., Ventura, O. N., Cousido-Siah, A., Haertlein, M., Joachimiak, A., Myles, D. A. A. & Podjarny, A. (2008). *Proc. Natl Acad. Sci. USA*, **105**, 1844–1848.
- Bon, C., Lehmann, M. S. & Wilkinson, C. (1999). *Acta Cryst.* **D55**, 978–987.
- Bouquiere, J. P., Finney, J. L., Lehmann, M. S., Lindley, P. F. & Savage, H. F. J. (1993). *Acta Cryst.* **B49**, 79–89.
- Budayova-Spano, M., Dauvergne, F., Audiffren, M., Bactivelane, T. & Cusack, S. (2007). *Acta Cryst.* **D63**, 339–347.
- Budayova-Spano, M., Fisher, S. Z., Dauvergne, M.-T., Agbandje-McKenna, M., Silverman, D. N., Myles, D. A. A. & McKenna, R. (2006). *Acta Cryst.* **F62**, 6–9.
- Campbell, J. W. (1995). *J. Appl. Cryst.* **28**, 228–236.
- Campbell, J. W., Hao, Q., Harding, M. M., Nguti, N. D. & Wilkinson, C. (1998). *J. Appl. Cryst.* **31**, 496–502.
- Chatake, T., Tanaka, I., Umino, H., Arai, S. & Niimura, N. (2005). *Acta Cryst.* **D61**, 1088–1098.
- Cipriani, F., Castagna, J. C., Wilkinson, C., Lehmann, M. S. & Buldt, G. (1996). *Neutrons in Biology*, edited by B. P. Schoenborn & R. B. Knott, pp. 423–431. New York: Plenum Press.
- Cipriani, F., Dauvergne, F., Gabriel, A., Wilkinson, C. & Lehmann, M. S. (1994). *Biophys. Chem.* **53**, 5–13.
- Coates, L., Erskine, P. T., Wood, S. P., Myles, D. A. & Cooper, J. B. (2001). *Biochemistry*, **40**, 13149–13157.
- Coates, L., Tuan, H. F., Tomanicek, S., Kovalevsky, A., Mustyakimov, M., Erskine, P. & Cooper, J. (2008). *J. Am. Chem. Soc.* **130**, 7235–7237.
- Cooper, S. J., Brockwell, D., Raftery, J., Attwood, D., Barber, J. & Helliwell, J. R. (1998). *Chem. Commun.*, pp. 1063–1064.
- Di Costanzo, L., Moulin, M., Haertlein, M., Meilleur, F. & Christianson, D. W. (2007). *Arch. Biochem. Biophys.* **465**, 82–89.
- Fisher, S. J. & Helliwell, J. R. (2008). *Acta Cryst.* **A64**, 359–367.
- Forsyth, V. T., Myles, D. A. A., Timmins, P. A. & Haertlein, M. (2001). *Opportunities for Neutron Scattering in the 3rd Millennium*, pp. 47–54. Grenoble: Institut Laue-Langevin.
- Gamble, T. R., Clauser, K. R. & Kossiakoff, A. A. (1994). *Biophys. Chem.* **53**, 15–26.
- Gardberg, A. S., Blakeley, M. P. & Myles, D. A. A. (2009). *Acta Cryst.* **F65**, 184–187.
- Gardberg, A. S., Del Castillo, A. R., Weiss, K. L., Meilleur, F., Blakeley, M. P. & Myles, D. A. A. (2010). *Acta Cryst.* **D66**, 558–567.
- Habash, J., Raftery, J., Nuttall, R., Price, H. J., Wilkinson, C., Kalb (Gilboa), A. J. & Helliwell, J. R. (2000). *Acta Cryst.* **D56**, 541–550.
- Hazemann, I., Dauvergne, M. T., Blakeley, M. P., Meilleur, F., Haertlein, M., Van Dorsselaer, A., Mitschler, A., Myles, D. A. A. & Podjarny, A. (2005). *Acta Cryst.* **D61**, 1413–1417.
- Helliwell, J. R., Habash, J., Cruickshank, D. W. J., Harding, M. M., Greenhough, T. J., Campbell, J. W., Clifton, I. J., Elder, M., Machin, P. A., Papiz, M. Z. & Zurek, S. (1989). *J. Appl. Cryst.* **22**, 483–497.
- Høghøj, P., Anderson, I. S., Ebisawa, T. & Takeda, T. (1996). *J. Phys. Soc. Jpn.* **65**, 296–298.
- Howard, E. I., Sanishvili, R., Cachau, R. E., Mitschler, A., Chevrier, B., Barth, P., Lamour, V., Van Zandt, M., Sibley, E., Bon, C., Moras, D., Schneider, T. R., Joachimiak, A. & Podjarny, A. (2004). *Proteins*, **55**, 792–804.
- Kossiakoff, A. A., Ultsch, M., White, S. & Eigenbrot, C. (1991). *Biochemistry*, **30**, 1211–1221.
- Kovalevsky, A. Y., Hanson, L., Fisher, S. Z., Mustyakimov, M., Mason, S. A., Forsyth, V. T., Blakeley, M. P., Keen, D., Wagner, T., Carrell, H. L., Katz, A. K., Glusker, J. P. & Langan, P. (2010). *Structure*, **18**, 688–699.
- Kovalevsky, A. Y., Katz, A. K., Carrell, H. L., Hanson, L., Mustyakimov, M., Fisher, S. Z., Coates, L., Schoenborn, B. P., Bunick, G. J., Glusker, J. P. & Langan, P. (2008). *Biochemistry*, **47**, 7595–7597.
- Leal, R. M. F., Teixeira, S. C. M., Blakeley, M. P., Mitchell, E. P. & Forsyth, V. T. (2009). *Acta Cryst.* **F65**, 232–235.
- Liu, X., Hanson, B. L., Langan, P. & Viola, R. E. (2007). *Acta Cryst.* **D63**, 1000–1008.

- Mason, S. A., Bentley, G. A. & McIntyre, G. J. (1984). *Neutrons in Biology*, edited by B. P. Schoenborn, pp. 323–334. New York: Plenum Press.
- Meilleur, F., Dauvergne, M.-T., Schlichting, I. & Myles, D. A. A. (2005). *Acta Cryst.* **D61**, 539–544.
- Meilleur, F., Snell, E. H., van der Woerd, M. J., Judge, R. A. & Myles, D. A. (2006). *Eur. Biophys. J.* **35**, 601–609.
- Myles, D. A. A. (2006). *Curr. Opin. Struct. Biol.* **16**, 630–637.
- Myles, D. A. A., Bon, C., Langan, P., Cipriani, F., Castagna, J. C., Lehmann, M. S. & Wilkinson, C. (1998). *Physica B*, **241–243**, 1122–1130.
- Niimura, N., Karasawa, Y., Tanaka, I., Miyahara, J., Kahashi, K., Saito, H., Koizumi, S. & Hidaka, M. (1994). *Nucl. Instrum. Methods A*, **349**, 521–525.
- Niimura, N., Minezaki, Y., Nonaka, T., Castagna, J. C., Cipriani, F., Hoghoj, P., Lehmann, M. S. & Wilkinson, C. (1997). *Nature Struct. Biol.* **11**, 909–914.
- Novak, W. R. P., Moulin, A. G., Blakeley, M. P., Schlichting, I., Petsko, G. A. & Ringe, D. (2009). *Acta Cryst.* **F65**, 317–320.
- Oksanen, E., Blakeley, M. P., Bonneté, F., Dauvergne, M. T., Dauvergne, F. & Budayova-Spano, M. (2009). *J. R. Soc. Interface*, **6**, S599–S610.
- Petit-Haertlein, I., Blakeley, M. P., Howard, E., Hazemann, I., Mitschler, A., Haertlein, M. & Podjarny, A. (2009). *Acta Cryst.* **F65**, 406–409.
- Petit-Haertlein, I., Blakeley, M. P., Howard, E., Hazemann, I., Mitschler, A., Podjarny, A. & Haertlein, M. (2010). *Acta Cryst.* **F66**, 665–669.
- Rausch, C., Bücherl, T., Gähler, R., von Seggern, H. & Winnacker, A. (1992). *Proc. SPIE*, **1737**, 255–263.
- Schoenborn, B. P. (1992). *Proc. SPIE*, **1738**, 92–198.
- Shu, F., Ramakrishnan, V. & Schoenborn, B. P. (2000). *Proc. Natl Acad. Sci. USA*, **97**, 3872–3877.
- Teixeira, S. C. M., Blakeley, M. P., Leal, R. M. F., Mitchell, E. P. & Forsyth, V. T. (2008). *Acta Cryst.* **F64**, 378–381.
- Tomanicek, S. J., Blakeley, M. P., Cooper, J., Chen, Y., Afonine, P. V. & Coates, L. (2010). *J. Mol. Biol.* **396**, 1070–1080.
- Tuominen, V. U., Myles, D. A. A., Dauvergne, M.-T., Lahti, R., Heikinheimo, P. & Goldman, A. (2004). *Acta Cryst.* **D60**, 606–609.
- Weiss, K. L., Meilleur, F., Blakeley, M. P. & Myles, D. A. A. (2008). *Acta Cryst.* **F64**, 537–540.
- Weiss, M. S. (2001). *J. Appl. Cryst.* **34**, 130–135.
- Wilkinson, C., Cowan, J. A., Myles, D. A. A., Cipriani, F. & McIntyre, G. J. (2002). *Neutron News*, **13**, 37–41.
- Wilkinson, C., Gabriel, A., Lehmann, M. S., Zemb, T. & Né, F. (1992). *Proc. SPIE*, **1737**, 324–329.
- Wilkinson, C. & Lehmann, M. S. (1991). *Nucl. Instrum. Methods A*, **310**, 411–415.
- Wilkinson, C., Lehmann, M. S., Meilleur, F., Blakeley, M. P., Myles, D. A. A., Vogelmeier, S., Thoms, M., Walsh, M. & McIntyre, G. J. (2009). *J. Appl. Cryst.* **42**, 749–757.
- Wlodawer, A. (1980). *Acta Cryst.* **B36**, 1826–1831.
- Wlodawer, A., Miller, M. & Sjölin, L. (1983). *Proc. Natl Acad. Sci. USA*, **80**, 3628–3631.
- Wlodawer, A. & Sjölin, L. (1982). *Proc. Natl Acad. Sci. USA*, **79**, 1418–1422.